

1 Dear Revisors,
2
3

4 We would like to thank you for your encouraging comments, which we largely agree upon. We are sure that the
5 manuscript will greatly benefit from your suggestions. Hereafter the list of your comments is reported, followed by our
6 response. We will also provide a version of the manuscript with the tracked revisions.
7

8 **Referee #1 comments:** in the Introduction section, when the Authors speaking about the use of innovative technologies
9 for the characterization and monitoring of landslide-affected areas (see from line 32 to line 38), including remote
10 sensing techniques and radar interferometry (both terrestrial and satellite), in according to scientific literature, the
11 authors should include some other references such as: Gullà et al., 2017; Peduto et al., 2017a; Tofani et al., 2014.

12 **Authors:** the proposed references were included.

13 **Referee #1** - in the section 3, at the line 131, the Authors speak in general about of a millimeter accuracy of the
14 acquired data by GB-InSAR. Give more detail about the real accuracy (range values). A comparison with conventional
15 ground monitoring techniques, was carried out? What are the differences on the accuracy also compared with the
16 InSAR data provided by satellite sensors? It might be useful to provide a comparison whit the values included in the
17 works of Nicodemo et al., 2016; Peduto 2017b; Casu et al., 2006) about the accuracy on the average velocities or
18 displacements data derived by satellite radar sensors processed by InSAR or DInSAR techniques.

19 **Authors:** More details about the range value accuracy were given in the text (including the suggested works).
20 References were also given in the discussion section about an automated total station working in the landslide area in
21 during our research (see the manuscript revised version).

22 **Referee #1** - in the section 5 as well as in the figures 7,9 and 10, the Authors refer to incremental cumulative
23 displacement (ICD) or monthly cumulated displacement (MCD) evaluated along the LOS direction. Why not along the
24 real movement direction? Could be performed a data projection? Please, provide further details about this.

25 **Authors:** It is well known that a GB-InSAR system is able to measure only the component of the movement parallel to
26 the LOS of the instrument. Thus the real displacement vector of the observed object can be calculated only if its
27 direction is a priori known. This is one of the major limits of the technique. This is why usually the instrument is set
28 with the view direction as parallel as possible to the expected deformations. The current paper was centered on the
29 application of a monitoring system applied to a particular case study (a debris-flow affected slope in a mountainous
30 inhabited area), which results could be shared with the involved technical personnel. Therefore we focused on easy
31 interpretable data, while the data projection on the slope in order to obtain of the real movement direction will be the
32 objective of a future work.

33 **Referee #1** - for a better understanding, an improvement of the Figures 3 and 11 is necessary. In particular, a visible
34 legend should be provided.

35 **Authors:** The legend of Figure 3 and 11 were improved.

36

37

Kindest regards

A handwritten signature in black ink, appearing to read "William Jodit". The signature is written in a cursive style with a large initial 'W' and 'J'.

38

39

40

41

42

43

44

45

46

47

48

49

50

51

52

53 ~~Emergency management of the 2010 Mt. Rotolon landslide by~~
54 ~~means of a local scale GB-InSAR monitoring system~~

55 "GB-InSAR monitoring of slope deformations in a mountainous
56 area affected by debris flow events"

57 William Frodella¹, Teresa Salvatici¹, Veronica Pazzi¹, Stefano Morelli¹, Riccardo Fanti¹

58 1. Department of Earth Sciences, University of Firenze, Via La Pira 4, 50121, Florence, Italy

59 *Correspondence to:* William Frodella (william.frodella@unifi.it)

60 **Abstract**

61 Diffuse and severe slope instabilities affected the whole Veneto region (Northeast Italy) between October 31st and
62 November 2nd 2010, following a period of heavy and persistent rainfall. In this context on November 4th 2010 a large
63 detrital mass detached from the cover of the Mt. Rotolon ~~dDeep sSeated gGravitational sSlope dDeformation~~ (DSGSD),
64 located in the upper Agno River Valley, channelizing within the Rotolon Creek riverbed and evolving into a highly
65 mobile debris flow. The latter phenomena damaged many hydraulic works, also ~~threatening putting at high risk~~ bridges,
66 local roads, together with ~~population the residents~~ of the Maltaure, Turcati and Parlati villages located along the creek
67 banks and ~~of~~ the Recoaro Terme town. ~~Starting Ffr~~ from the beginning of the emergency phase, the Civil Protection
68 system was activated, involving the National Civil Protection Department, Veneto Region, ~~and local administrations~~
69 personnel and technicians, as well as scientific institutions. On December 8th 2010 a local scale monitoring system,
70 based on a ~~gGround bBased iInterferometric sSynthetic aAperture rRadar~~ (GB-InSAR), was implemented in order to
71 evaluate the slope deformation pattern evolution in correspondence of the debris flow detachment sector, with the final
72 aim of assessing the landslide residual risk and manage the emergency phase. This paper describes the ~~resultsouteomes~~
73 of a two years GB-InSAR monitoring campaign (December 2010 - December 2012), its application for monitoring,
74 mapping, and emergency management activities, in order to provide a rapid and easy communication of the results to
75 the involved technicians and civil protection personnel, for a better understanding of the landslide phenomena and ~~the~~
76 decision-making process in a critical landslide scenario.

77
78 **1 Introduction**

79 Deep ~~sSeated gGravitational sSlope dDeformations~~ (DSGSD) are normally not considered hazardous phenomena, due
80 to their typically very slow evolution; nevertheless under certain conditions ground movements can accelerate evolving
81 into faster mass movements, ~~which may favour or favoring~~ collateral landslide processes (Crosta, 1996; Crosta and
82 Agliardi, 2003). Therefore, a multidisciplinary approach is fundamental in order to understand the complex nature of
83 such phenomena, ~~so as to with the aim of~~ assessing the correct mitigation measures. In this framework advanced
84 mapping methods, based on spaceborne, aerial and terrestrial remote sensing platforms, represent the optimal solution
85 for landslide detection, monitoring and mapping; in ~~variousdifferent~~ physiographic and land cover conditions, ~~with~~
86 ~~special regards particularly with~~ large phenomena and hazardous non accessible sectors (Casagli, 2017b; Guzzetti et
87 al., 2012). In ~~recentthe last~~ decades, many advanced remote sensing technologies have ~~gained widespread~~
88 ~~recognitionbeen increasingly being recognized~~ as efficient remote surveying techniques for the characterization; and

89 monitoring of landslide-affected areas, in terms of resolution, accuracy, data visualization, management, and
90 reproducibility. ~~Among these are, such as:~~ digital photogrammetry (Chandler, 1999; Zhang et al., 2004), laser scanning
91 (Abellan et al., 2006; Gigli et al., 2012, 2014c; Jaboyedoff et al., 2012; Tapete et al., 2012), Infrared Thermography
92 (Teza et al., 2012; Gigli et al. 2014a, b; Frodella et al., 2015) and radar interferometry, both terrestrial and satellite (Luzi
93 et al., 2004; Bardi et al., 2014; Tofani et al., 2014; Ciampalini et al., 2016; Gullà et al., 2017; Peduto et al., 2017a).

94 Ground ~~b~~Based ~~i~~nterferometric ~~s~~ynthetic ~~a~~perture ~~r~~adar (GB-InSAR) systems in particular, for their ~~e~~apability
95 ~~to~~of ~~measur~~eing displacements with high geometric accuracy, temporal sampling frequency, and adaptability to specific
96 applications (Monserrat et al., 2014), represent powerful devices successfully employed in: a) engineering and
97 geological applications for detecting structural deformation, and surface ground displacements (Tarchi et al., 1997;
98 2003; Antonello et al., 2004; Casagli et al., 2010; 2017a), b) for the monitoring of volcanic activity (Nolesini et al.,
99 2013; Di Traglia et al., 2014a, b), ~~and~~ c) for analysing the stability of historical towns built on isolated hilltops (Luzi et
100 al., 2004; Frodella et al., 2016; Nolesini et al., 2016). Furthermore, in ~~the~~ recent years GB-InSAR technique has
101 developed to an extent where it can significantly contribute to the management of major technical and environmental
102 disasters (Del Ventisette et al., 2011; Broussolle et al., 2014; Lombardi et al., 2017; Bardi et al., 2017a, b). Between
103 October 31st 2010 and November 2nd 2010 the whole Veneto region territory (north-eastern Italy; Fig. 1) was hit by
104 heavy and persistent rainfall, that ~~diffusely~~ triggered widespread floodings and abundant slope failures, causing
105 ~~extensivewidespread~~ damages to people (3 fatalities and about 3500 evacuated people) and structures., not to mention
106 furthermore resulting in heavy economic losses infor the agricultural, livestock, and industrial activities.

107 In this context on November 4th 2010, part of detrital cover of the Rotolon DSGSD suffered the detachment of a mass
108 approximately 320000 m³ in volume, thatwhich channelized in the Rotolon Creek bed causing a large debris flow. This
109 phenomenon was characterized by more than three kilometres of run-out ~~distance~~, damaging various hydraulic works
110 ~~and infrastructures~~ (creek dams, weirs, bank protections), and threatening putting at high risk the various
111 structuresinfrastructures (bridges, local roads, houses); together with ~~the population of the inhabited areas located~~
112 nearby the creek banks (those residing in the villages of Maltaure, Turcati, Parlati and the town of Recoaro Terme; Fig.
113 1).

114 On December 8th 2010 a GB-InSAR monitoring system was implemented in order to assess the landslide residual
115 displacements and support the local authorities infor the emergency management (Fidolini et al., 2015), calling into
116 play. In this framework the Civil Protection system was activated in order to manage the landslide emergency phase, by
117 involving the both the national (DPC) and regional (DPCR) ~~c~~Civil ~~p~~rotection ~~d~~epartments, in cooperation with
118 scientific institutions (namely “~~c~~Competence centres”, CdCs), local administration personnel, and technicians
119 (Bertolaso et al., 2009; Pagliara et al., 2014; Ciampalini et al., 2015). Accurate geomorphological field surveys were
120 also carried out in this phase, in order to analyse the landslide morphological features ands to improve the radar data
121 interpretation (Frodella et al., 2014; 2015; 2017). In addition, a 3D landslide 3D runout numerical modelling
122 performed towith the aim of identifying the source and impact areas of potentialssible debris flow events ~~source and~~
123 impacted areas, flow velocity and deposit distribution within the Rotolon creek valley (Salvatici et al., 2017).

124 This workpaper is focused on the outeomes results of a long-term continuous GB-InSAR monitoring campaign
125 (December 2010 - December 2012) carried out during the post-event recovery phase, in which monitoring, mapping,
126 and emergency management activities were implemented tofor assessing the landslide residual risk and analyse its
127 kinematics. In this contextframework field activities were carried out by local Civil Protection operators and technicians
128 for a validation of the remotely sensed data (landslide area inspections). In particular, the analysed radar data were

129 shared with the ~~involved~~ technicians and civil protection personnel ~~involved~~ in order to provide a rapid and easy
 130 communication of the results, and enhance the synergy ~~of with~~ all ~~of~~ the subjects involved in the recovery phase.

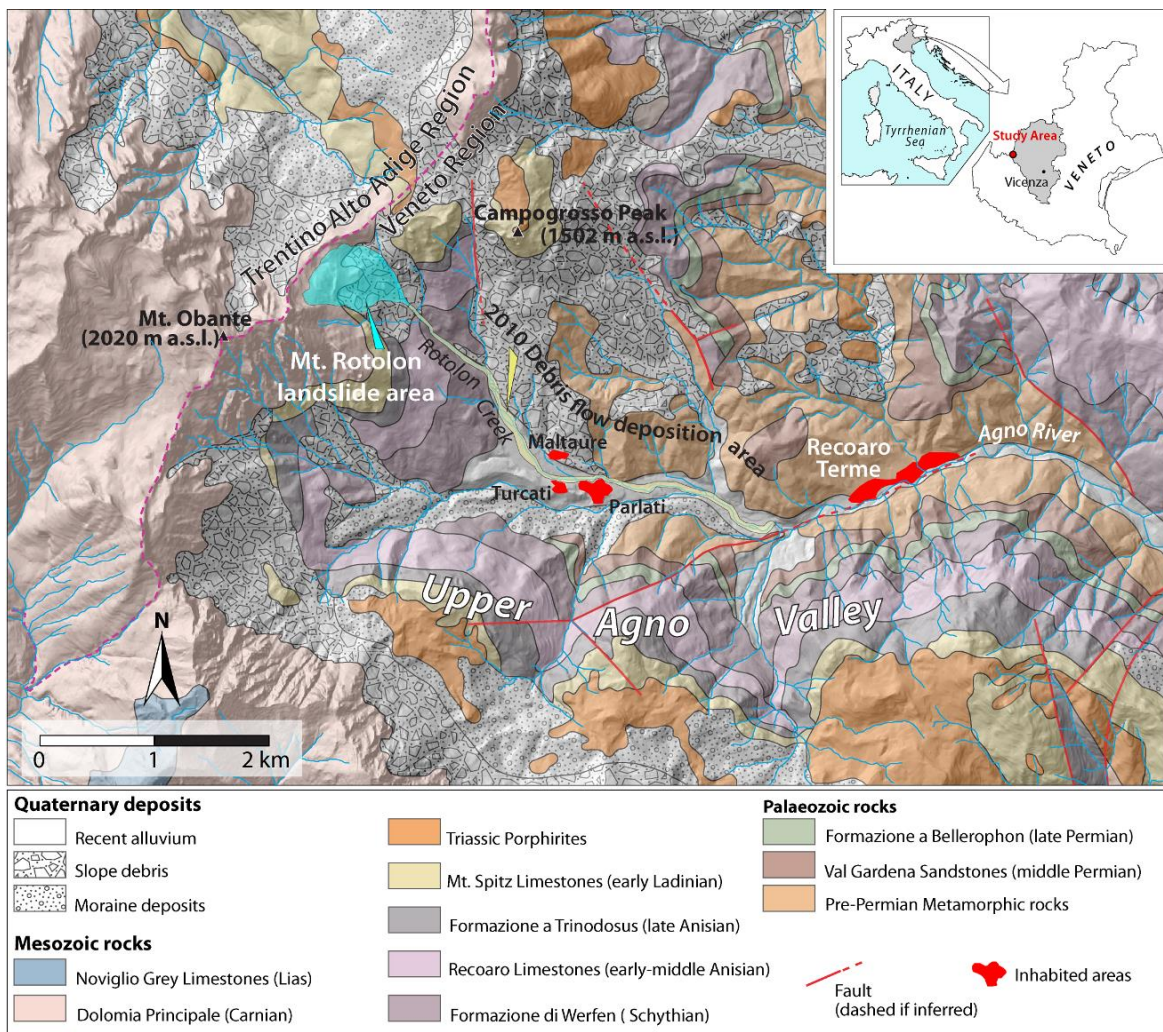
131

132 **2. Study area**

133 The Rotolon DSGSD is located in the Vicentine Prealps, on the south-eastern flank of the Little Dolomites chain, in the
 134 uppermost Agno river valley (Fig. 1). The instability processes of the ~~area valley~~, such as slope failures and debris flows
 135 induced as secondary phenomena of the DSGSD, have threatened the ~~u~~Upper Agno valley for centuries (Frodella et al.,
 136 2014).

137 From a geological point of view the landslide develops in the uppermost portion of a ~~mainly dolomitic-limestone~~
 138 ~~stratigraphic succession~~, sub-horizontally bedded ~~mainly dolomitic limestone stratigraphic succession~~, from middle
 139 Triassic to lower ~~J~~Jurassic in age, belonging to the South Alpine Domain (De Zanche and Mietto, 1981).

140



141

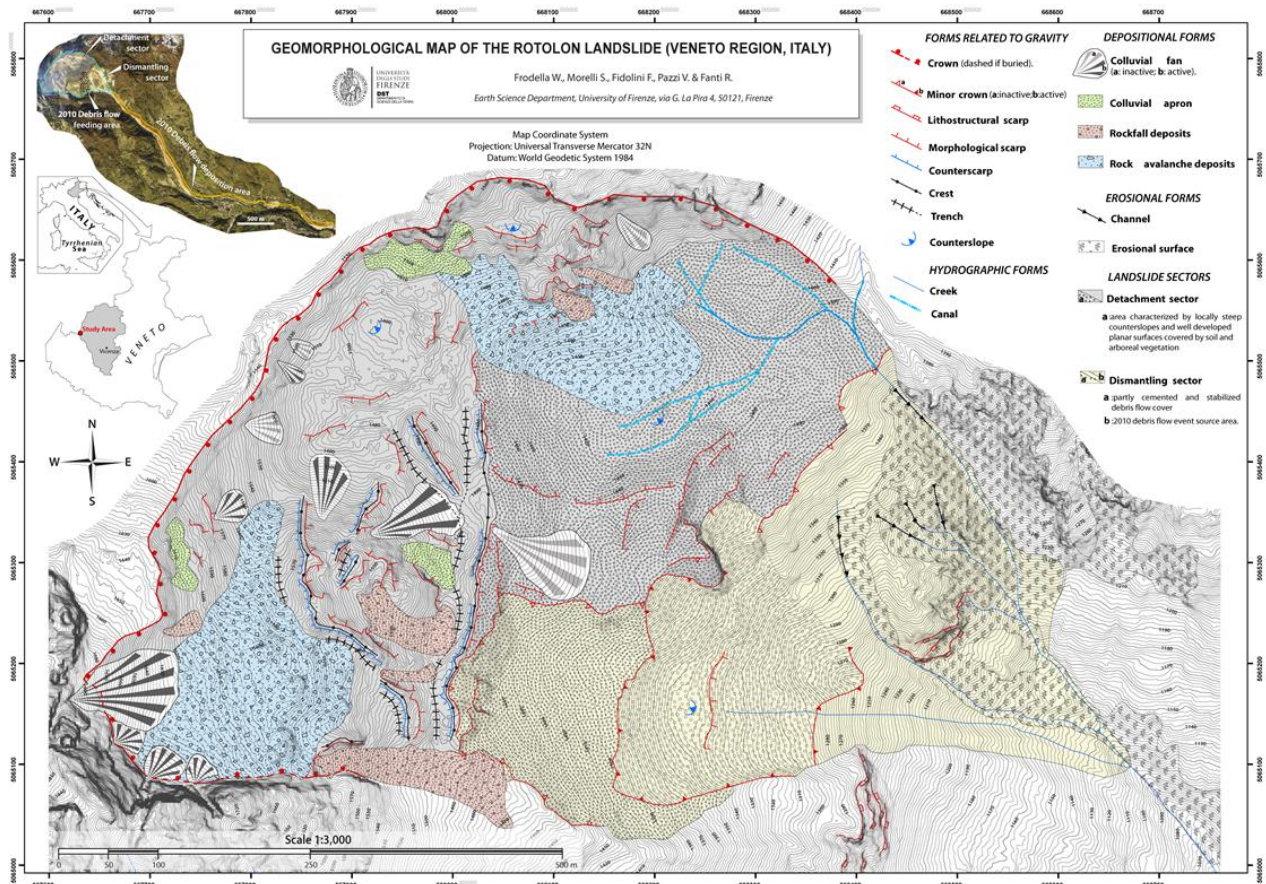
142 **Figure 1.** Geological sketch map of the Upper Agno River Valley with the location of the Rotolon landslide.

143 The mass movement is delimited to the NW by the ridge of the Mount Obante group and develops from about 1700 to
 144 1100 m a.s.l., covering an area of 448000 m². The Rotolon DSGSD can be classified as a DSGSD (“~~s~~Sackung type”;
 145 Zischinsky, 1969), and ~~it is~~ characterized by a complex activity (Cruden and Varnes, 1996) ~~causing that leads to~~ a rough
 146 ~~morphology physiographic, characterized by with~~ steep scarps, trenches, crests and counterscarps (Figs. 2 and 3).

147 Two distinct sectors can be identified, based on the ~~acting~~ dominant slope instability processes ~~in act~~: i) an upper
 148 “~~d~~Detachment sector”, followed downstream by a ii) “~~d~~Dismantling sector” (Frodella et al., 2014). The ~~d~~Detachment
 149 sector (~~with having~~ a mean slope of 30°), develops downstream ~~of~~ from the main landslide crown (Figs. 2a and b; Fig. 3),
 150 and ~~it is~~ dominated by extensional deformation ~~causing that leads to~~ the development of tensional fractures, resulting in
 151 alternate trenches and crests ~~creating which creates a~~ very rough, stepped topographic surface. This area is affected ~~both~~
 152 by gravitational and erosional processes, ~~as well as and by~~ the rock mass detensioning and disaggregation, ~~resulting~~
 153 ~~in which cause~~ the accumulation of various depositional elements (colluvial fans, colluvial aprons, rock fall and rock
 154 avalanche deposits) formed by very coarse ~~and~~ heterometric clasts, ranging from cobbles to boulders with scattered
 155 blocks (decimetric to decametric in size) in a coarse sandy matrix (Figs. 3 and 4).
 156 The ~~d~~Dismantling ~~sector area~~ (mean slope of 34°) includes sectors formed by ~~sub-vertical~~ highly weathered ~~sub-vertical~~
 157 rock walls. It is dominated by surf~~ace~~icial processes (e.g., concentrated and diffuse erosion, slope-waste deposition due
 158 to gravity, detrital cover failures) that ~~widely substantially~~ cover the evidences of deeper deformations (Figs. 3 and 4).
 159 ~~This area~~ ~~Dismantling sector~~ supplies material for debris flows, which channelize downstream within the Rotolon
 160 ~~c~~Creek bed, ~~therefore~~ representing the most critical sector ~~for with respect to~~ short-term hazardous phenomena.
 161

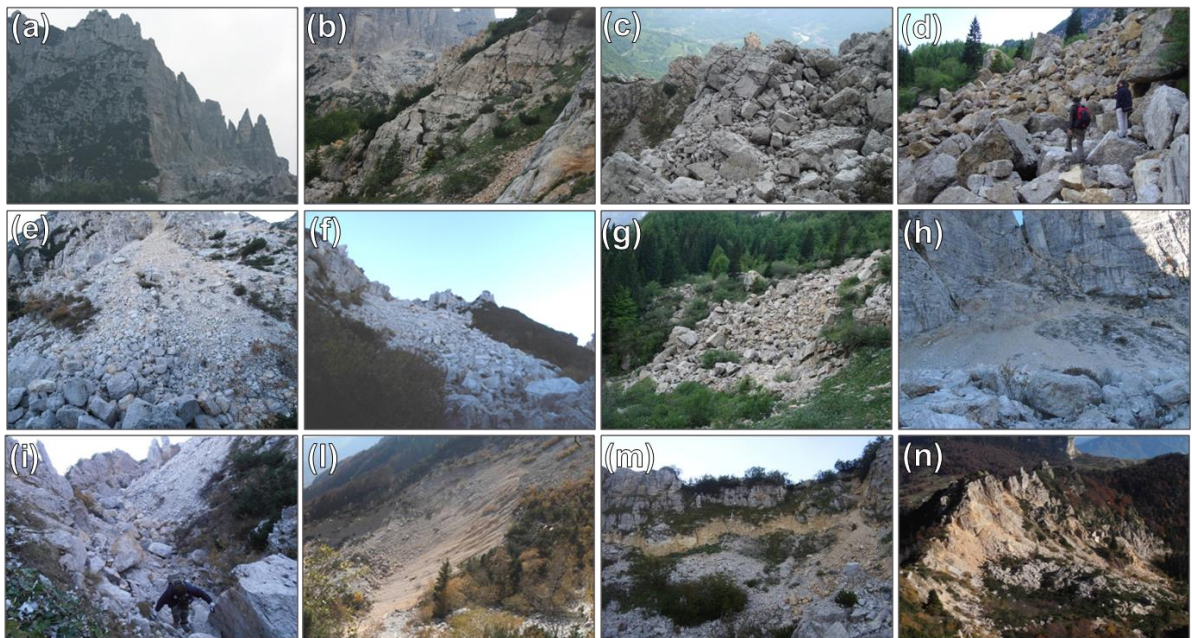


162
 163 **Figure 2.** The Mt. Rotolon DSGSD plan (a); landslide sectors (b, c) and the 2010 debris flow features (d, e).



164
165

Figure 3. Geomorphological map of the Rotolon Landslide (modified after Frodella et al., 2014).



166

167 **Figure 4.** Geomorphic and sedimentary features of the Mt. Rotolon DSGSD: **(a)** Detachment sector: **(a)** rock walls prone
168 to rock falls; **(b, c)** rock mass affected by different stages of disaggregation; **(d)** plurimetric rock blocks within rock
169 avalanche deposit. Main depositional elements within the landslide body: **(e)** colluvial fan; **(f, g)** channelized and
170 diffused rock fall deposits; **(h)** colluvial aprons. Main landslide linear elements: **(i)** landslide trench; **(l)** 2010 debris
171 flow detachment scarp; **(m)** DSGSD crown sector; **(n)** landslide crest.

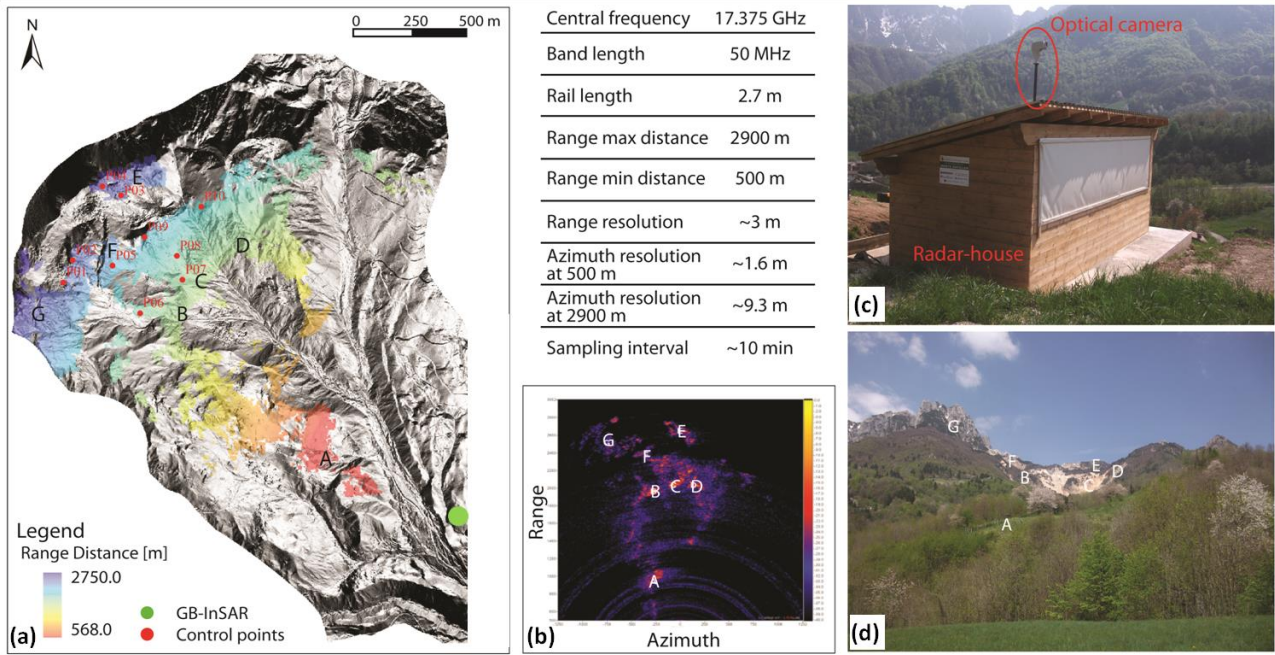
172 3. The GB-InSAR technique basic theoretical principles

173 The GB-InSAR is a computer-controlled microwave transmitting and receiving antenna, that moves along a mechanical
174 linear rail in order to synthesize a linear aperture along the azimuth direction (Tarchi et al., 1997). ~~The device~~ radiates
175 ~~an area with~~ microwaves in the Ku band (12-18 GHz) and registers the backscattered signal in the acquiring time
176 interval (~~from few to~~ less than 1 minute with the most modern systems). Each acquisition produces a complex matrix
177 of values from which phase and amplitude information are calculated (Luzi et al., 2004; Luzi, 2010). A SAR image
178 contains amplitude and phase information of the observed objects' backscattered echo within the investigated scenario,
179 and it is obtained by combining the spatial resolution along the direction perpendicular to the rail (range resolution,
180 ΔR_r) and the one parallel to the synthetic aperture (azimuth or cross-range resolution, ΔR_{az}) (Luzi, 2010). The working
181 principle of the GB-InSAR technique is the evaluation of the phase difference, pixel by pixel, between two pairs of
182 averaged sequential SAR complex images, which ~~form~~ constitutes an interferogram (Bamler and Hartl, 1998). The
183 latter does not contain topographic information, given the antennas fixed position during different scans (zero baseline
184 condition). Therefore, in the elapsed time between the acquisition of two or more subsequent coherent SAR images, it is
185 possible to derive from the obtained interferograms a 2D map of the displacements that occurred along the sensor LOS
186 (~~with a millimeter accuracy in the Ku band~~) (Tarchi et al., 1997; 2003; Pieraccini et al., 2000; 2002). The capability of
187 InSAR to detect ground displacement depends on the persistence of phase coherence (ranging from 0 to 1) over
188 appropriate time intervals (Luzi, 2010). Among the technique's advantages ~~it should be highlighted it must be noted~~ that
189 GB-InSAR works: a) without any physical contact with the slope, avoiding the need of accessing the area; b) in almost
190 ~~every~~ any light and atmospheric condition; c) continuously over a long time; d) with ~~a~~ millimetric accuracy ~~(the~~
191 ~~accuracy of the measured phase is usually a fraction of the operated wavelength; Luzi, 2010)~~; e) providing ~~extensive~~
192 ~~and detailed~~ near real time ~~detailed and spatially extensive~~ information.

193 This latter feature in particular gives a strong advantage with respect to traditional ground surface methods (like
194 inclinometers, extensometers, total stations), which on the contrary provide single-point information, ~~and are~~ generally
195 ~~are~~ not sufficient to evaluate the kinematics and ~~potential~~ behaviour of ~~a~~ complex landslide. The main drawback of the
196 technique is the logistics of the installation platform, both because the GB-InSAR system measures only the
197 displacement component parallel to the line of sight (L.O.S.), and because the azimuth resolution (the ability to separate
198 two objects perpendicular to the distance between the sensor and the target) ~~lessens~~ reduces with the increase of the
199 distance ~~with respect to~~ from the target (Fig. 5). Moreover, vegetated areas can be another drawback of the technique
200 since they are commonly characterized by ~~signal~~ low coherence and power intensity.

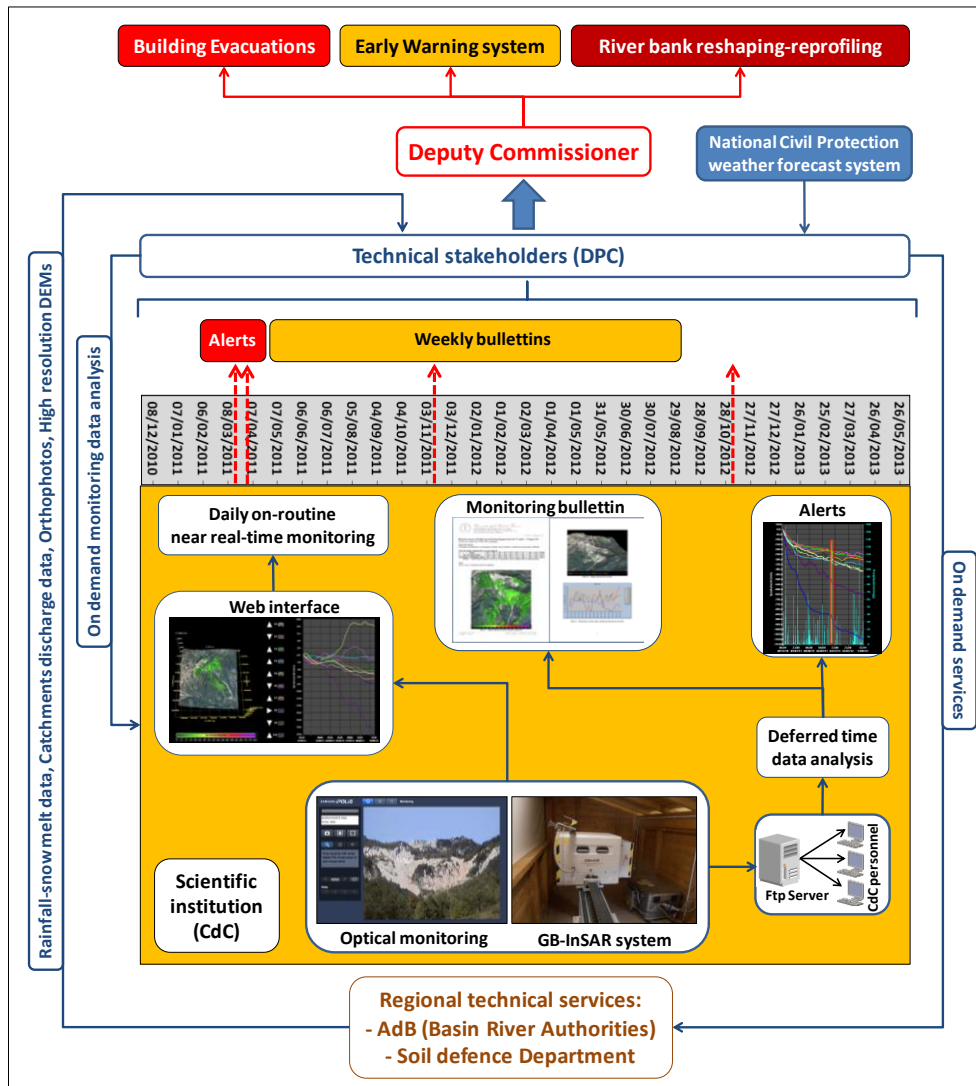
201 4. The adopted monitoring system

202 The GB-InSAR system was installed in the Maltaure village, at an average distance of 3 km ~~with respect to~~ from the
203 landslide, pointing upwards to NW (Fig. 5). The radar parameters are summarized in Fig. 5. Given the acquisition
204 setting of the site and the civil protection ~~needs~~ purposes, the radar data covers an area of 1.2 km². The logistics of the
205 GB-InSAR system installation favored a good spatial coverage of the data on the monitored area, especially with
206 ~~special~~ regards to the ~~d~~ dismantling sector. Nevertheless, shadowing effects, due to the slope roughness, crests and
207 counter-slope surfaces affect the ~~d~~ detachment sectors (Figs. 5 and 7).



208
209 **Figure 5.** The adopted monitoring system: (a) Location of the GB-InSAR system and radar data coverage features (A-
210 G=recognized landslide sectors); (b) the adopted monitoring parameters and radar power image, displaying the
211 correspondent recognized landslide sectors; (c) the radar system hut setting; (d) picture of the monitoring optical system
212 scenario (A-G=corresponding sectors).

213 The radar system acquired GB-InSAR data every 10 minutes, from which cumulated 2D displacement maps, and
214 displacements time series of 10 measuring points (Fig. 5) were obtained. GB-InSAR data were processed using
215 LiSALab software (Ellegi s.r.l.) and uploaded via LAN network: i) on a dedicated Web-based interface, allowing for a
216 near real time data on-routine visualization; ii) on a remote ftp server (in ASCII format), in order to perform on demand
217 analysis in case of critical weather events ~~forecast by~~based on the national civil protection weather ~~forecast~~ system (Fig.
218 6). The latter were performed integrating into a GIS environment the displacement maps and comparing them with
219 ancillary data (rainfall, geological and geomorphological maps). In addition, a remotely adjustable robotized high
220 resolution optical camera (Ulisse Compact model produced by Videotec S.p.A, digital zoom 10x - 36x),
221 ~~manouverable~~ageable via IP-Ethernet interface, was installed in correspondence ~~withof~~ the radar system, acquiring data
222 every 60 minutes and allowing for programmable zooms. ~~The objective of this device waswith the aim of to~~ checking of
223 the ~~landslide~~-hazardous and inaccessible Dismantling sector ~~of the landslide~~ (Figs. 5 and 6). The time line rationale of
224 the monitoring system and emergency management procedures is summarized in Fig. 6.



225

226

Figure 6. Time line rationale of the Rotolon monitoring system and emergency management procedures.

227

5. GB-InSAR data analysis

228

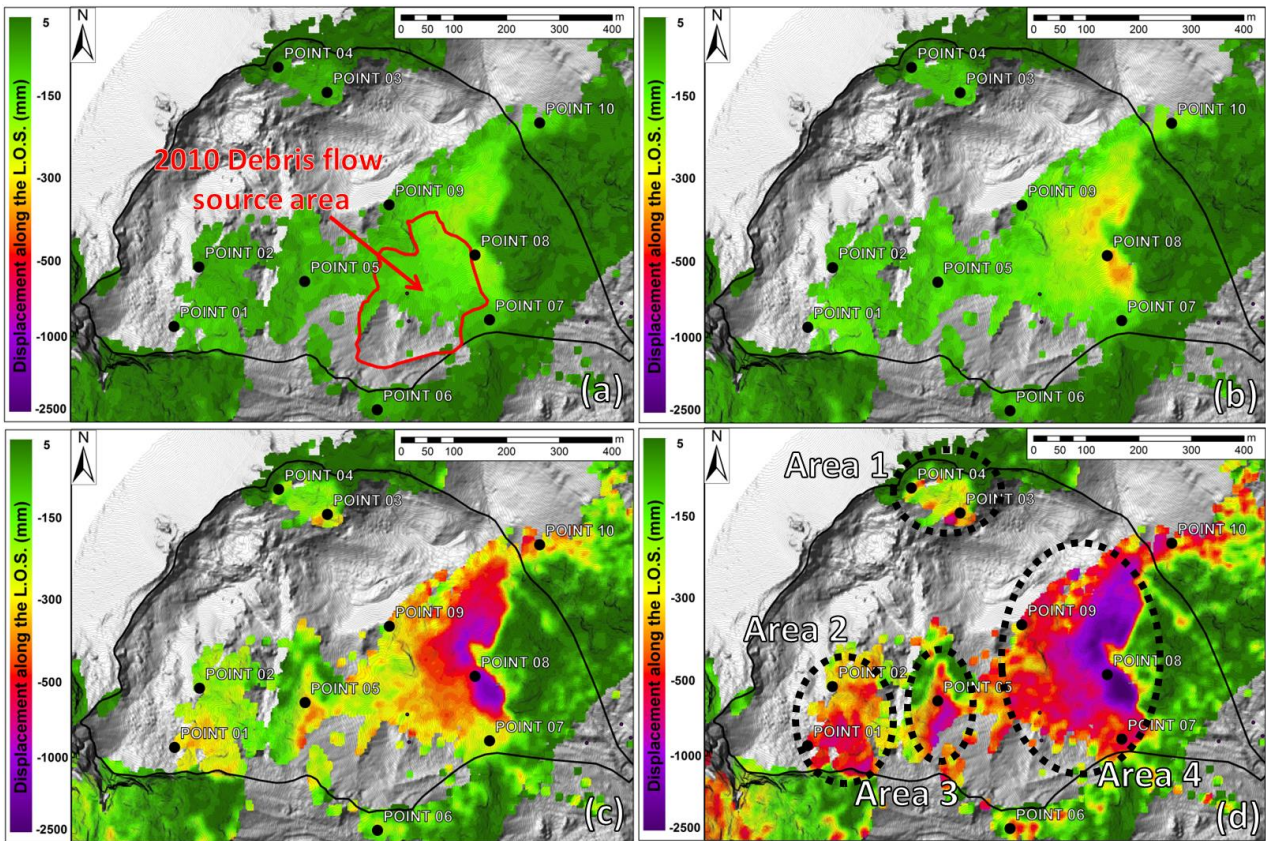
The obtained GB-InSAR incremental cumulative displacement (ICD) maps and the displacement time series of the measuring points obtained displacement time series are shown in Figs. 7 and 8, respectively. By using a selected colour scale, the obtained radar maps obtained are displayed as a function of the displacement measured in the period covered by the acquisitions, spanning from December 8th 2010 up to the beginning of each month of the monitoring campaign, until the end of the monitoring period (the negative displacement values indicate movements approaching to the sensor; Fig. 7). In order to evaluate the deformation rates and provide an easily-interpretable data, a traffic light-type colour scale was applied in all the displacement maps.

234

235

GB-InSAR measuring points (corresponding to a 5 x 5 pixel size area) were selected in correspondence with sectors where the radar signal is characterized by high stability, in order to monitor the landslide kinematics and characterize the various landslide physiographic features (Fig. 7). Furthermore with the aim of performing a temporally detailed displacement analysis and detecting the spatial pattern of residual landslide deformation, monthly cumulated displacement (MCD) maps were also selected and analysed from the collected GB-InSAR dataset (Fig. 9).

239

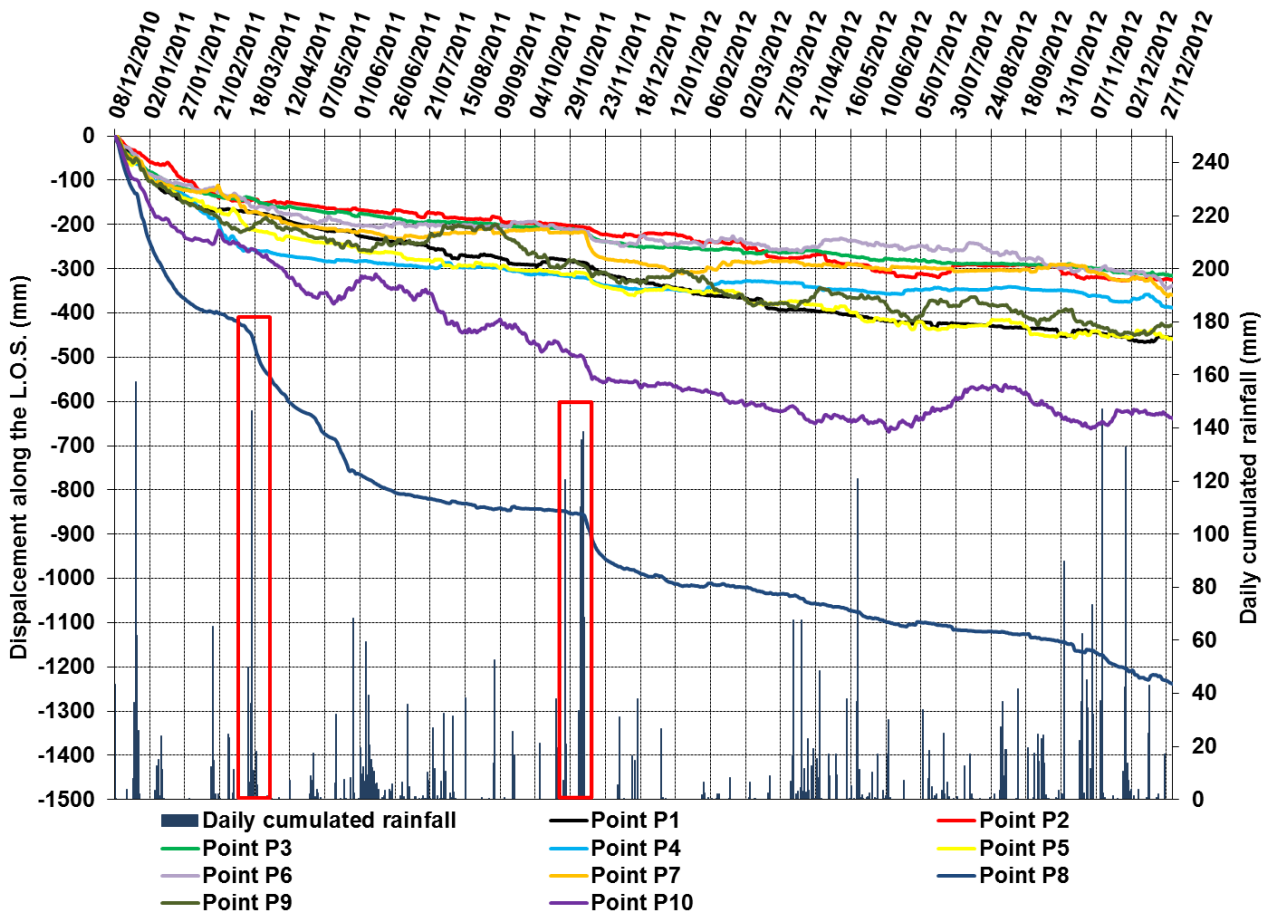


240
 241 **Figure 7.** ICD maps of the Rotolon landslide: (a) December 8th 2010 - January 1st 2011; (b) December 8th 2010 -
 242 February 1st 2011; (c) December 8th 2010 - December 1st 2011; (d) December 8th 2010 - December 31st 2012 (Point 1-
 243 10 represent the GB-InSAR measurement points in correspondence of which the displacement time series were
 244 extracted).

245 From the analysis of the collected GB-InSAR dataset of the ICD maps (Fig. 7) four distinct areas characterized by
 246 relevant residual cumulated displacement were identified (Fig. 7d):

- 247 - Area 1 (ICD=737 mm, about 12500 m² in extension) and Area 2 (ICD=751 mm, area of 28000 m²), corresponding to
 248 the material infilling the ~~d~~Detachment sector (Fig. 2), such as minor rock fall and rock avalanche deposits;
- 249 - Area 3 (ICD=960 mm; 12000 m² in extension) and Area 4 (ICD=2437 mm; 88000 m² coverage), both falling within
 250 the ~~d~~Dismantling sector detrital cover (Fig. 2) which was not affected by the 2010 debris flow detachment.

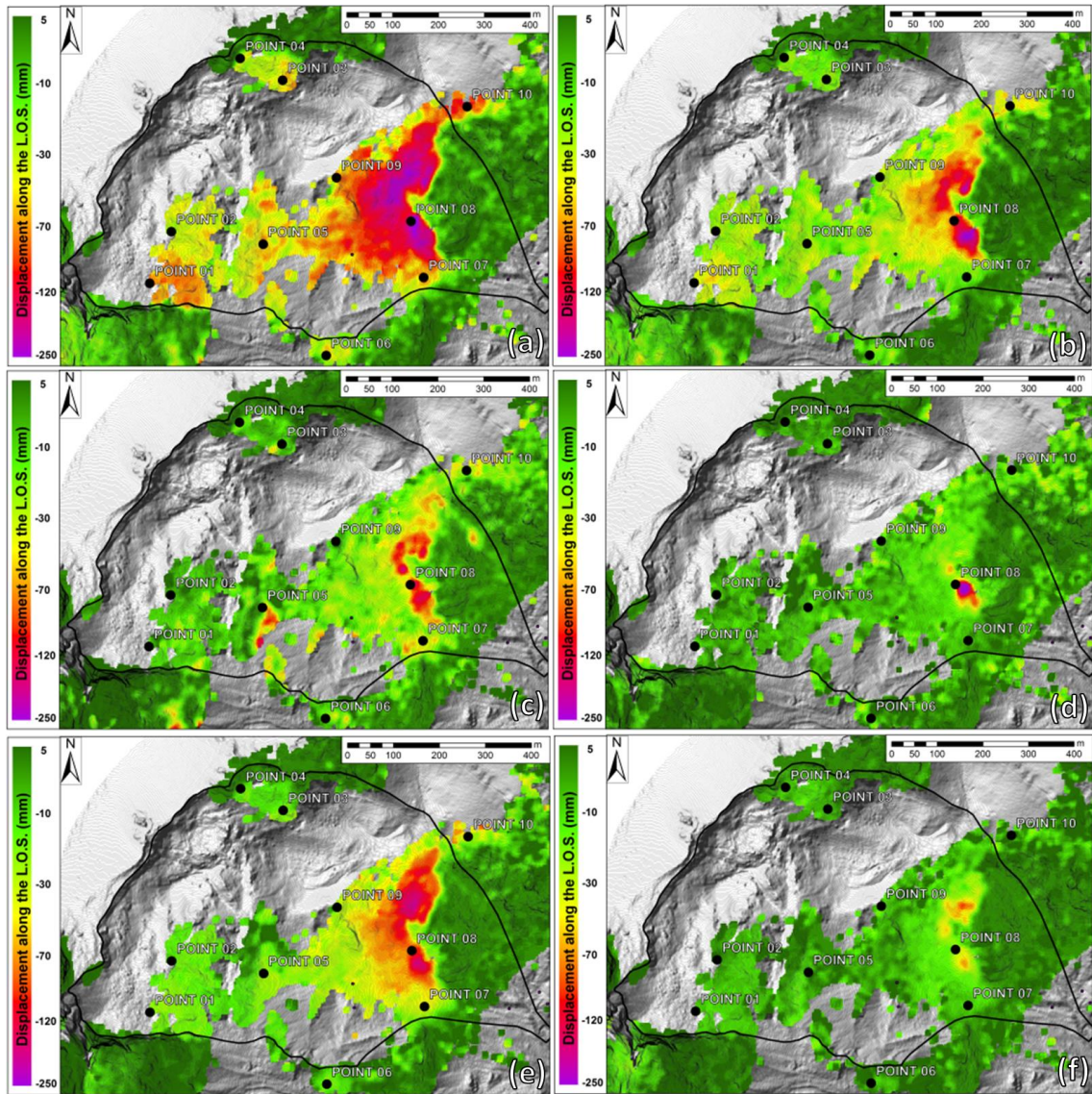
251 The measuring points time series (Fig. 8) display cumulated displacements ranging from 337 mm (Point 6) to 595 mm
 252 (Point 4, located in Area 1); Point 8 in particular (falling within Area 4) displays the monitored area cumulated peak
 253 displacements (ICD=1476 mm), showing two acceleration periods (middle March 2011 and beginning of November
 254 2011), alternating with a more linear trend. The comparison amongst the MCD maps highlighted a first phase of
 255 widespread residual displacements (December 2010, Fig. 9a), which gradually decreased ~~starting~~ starting from the following
 256 month (Fig. 9b). In the ~~subsequentfollowing~~ subsequent following period ground deformation took place in correspondence ~~with~~ with
 257 limited sectors within Area 4 (May 2011 in particular shows ~~the~~ the higher MCD up to 244 mm; Fig. 9d), except for a widespread
 258 reactivation recorded in November 2011 (Fig. 9e).



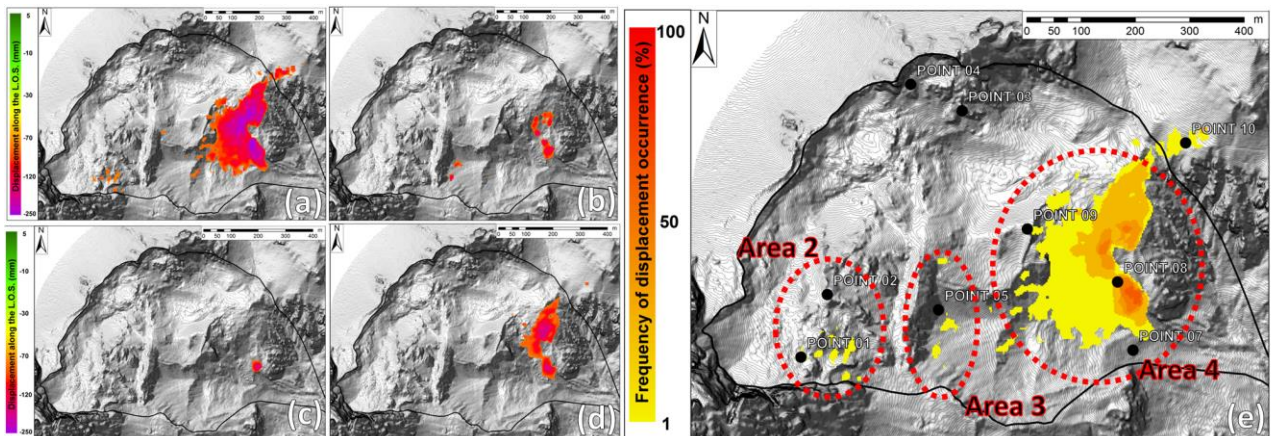
259

260 **Figure 8.** Selected measuring points displacement time series of the monitored scenario (red squares enhance Point 8
 261 accelerations).

262 Furthermore, in order to automatically extract the most hazardous residual displacement sectors, the MCD dataset was
 263 analysed by means of a MATLAB code (Salvatici et al., 2017) (Fig. 10). The code extracts from the dataset all of the
 264 areas affected by deformation higher than a selected threshold value, set equal to 92.3 mm, being the minimum
 265 displacement among all the maximum MCD values. The results are displacement maps showing only the areas with
 266 such selected displacements (Fig.10 a-d), confirming the trend highlighted by the MCD maps (Fig. 9). The second
 267 operation of the employed code consists in the frequency calculation of the displacement occurred (the code computes
 268 how many times each pixel has recorded the selected displacement during the monitoring period) (Fig. 10e). By using
 269 this method, three critical areas characterized by repeated residual reactivations were detected: Area 2, Area 3 (1
 270 reactivation) and especially Area 4 (8 reactivations).



271
 272 **Figure 9.** Selection of MCD maps from the GB-InSAR dataset: (a) December 2010 (232 mm cumulated peak
 273 displacement); (b) January 2011 (214 mm); (c) March 2011 (173 mm); (d) May 2011 (244 mm); (e) November 2011
 274 (174 mm); (f) November 2012 (106 mm).



275
 276 **Figure 10.** Residual reactivation maps obtained from selected MCD maps by means of the employed MATLAB code
 277 analysis: (a) December 2010; (b) March 2011; (c) May 2011; (d) November 2011; (e) frequency map of the reactivation
 278 of the critical residual displacement sectors, classified based on their activation frequency.

279 6. Discussion

280 Successful strategies for landslide residual hazard assessment and risk reduction would imply integrated
281 methodologies for instability detection, mapping, monitoring, and forecasting (Confuorto et al., 2017). In order to
282 provide information on the nature, extent and activation frequency of ancient landslides, standard detection and
283 mapping procedures need a combination of field-based studies and advanced techniques, such as remote sensing data
284 analysis and geophysical investigations (Ciampalini et al., 2015; Lotti et al., 2015; Del Soldato et al., 2016; Morelli et
285 al., 2017; Pazzi et al., 2017a, b). In ~~this context~~ particular GB-InSAR represents a versatile and flexible technology,
286 allowing for rapid changes in the type of data acquisition (geometry and temporal sampling) based on the characteristics
287 of the monitored slope failure, which is capable of assessing the extent and the magnitude of the landslide residual
288 hazard (Di Traglia et al., 2014; 2015; Carlà et al., 2016a, b). In the presented case study the 2 year continuous GB-
289 InSAR monitoring campaign ~~made it possible~~ allowed to measure the slope displacement with ~~a~~ millimetric accuracy
290 over a 1.2 km square landslide area, enabling ~~the~~ analyses of the evolution pattern ~~connected to~~ the landslide
291 residual hazard. The measured deformation pattern is consistent, in terms of extent and values, with the results obtained
292 by an automated total station monitoring network, working approximately in parallel with the GB-InSAR system
293 (Frigerio et al., 2014; Bossi et al., 2015).

294 By comparing the landslide geomorphological map (Frodella et al., 2014) with the ICD displacement map of whole
295 monitored period (Fig. 11), the four critical areas shown in Figure 7 are analysed in detail:

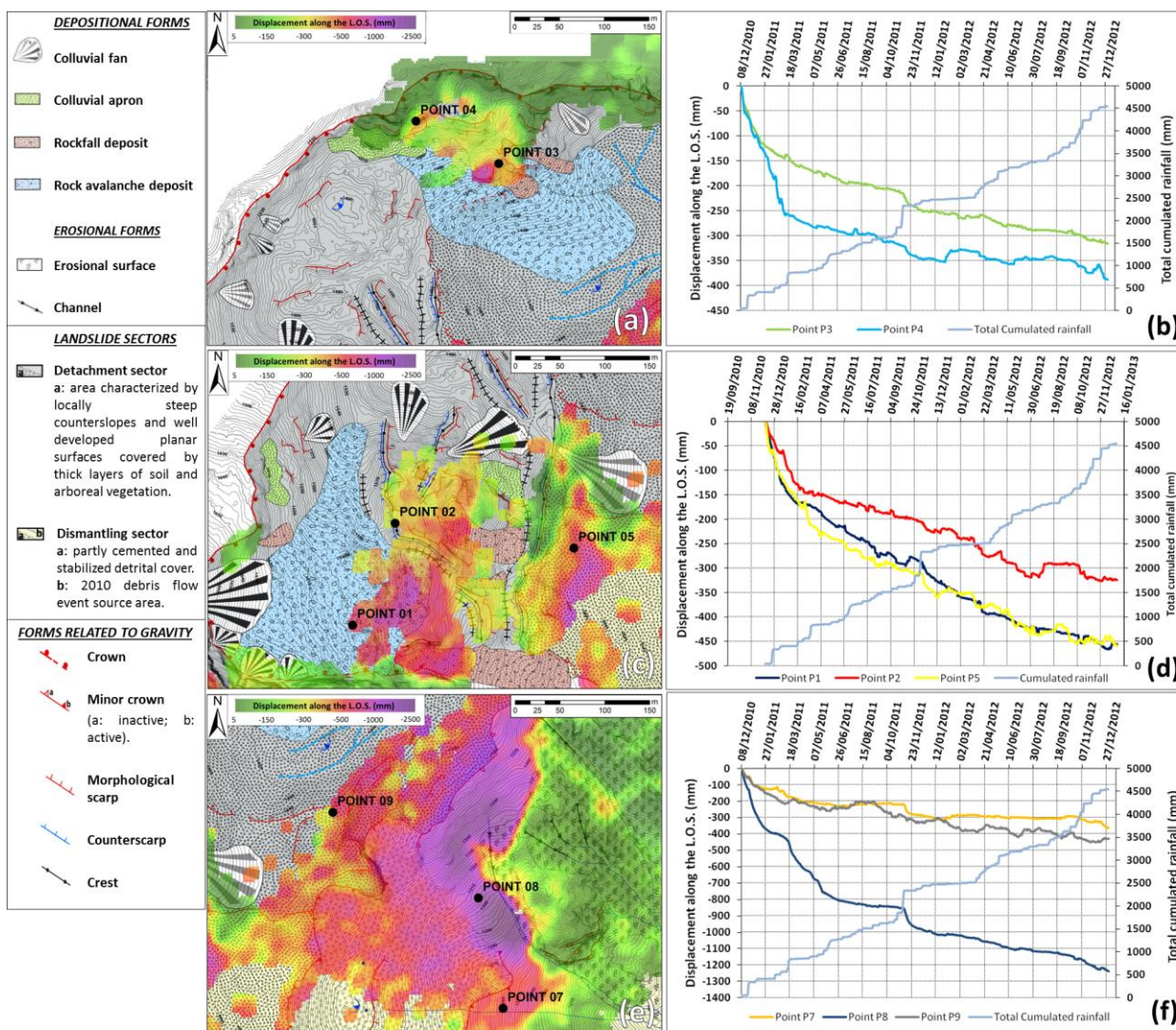
296 - Area 1, including measuring Points 3 and 4, is located in the northern side of ~~d~~Detachment sector (Fig. 11a). In the
297 first few months (between December 2010 and March 2011) ~~t~~The points recorded ~~in the first few months (between~~
298 ~~December 2010 and March 2011)~~, a peak of displacements of about 260 mm (Point 4) and 150 mm (Point 3);
299 after this period the displacement decreased up to 8th November 2011. Between November 8th and 12th ~~November~~, during a major
300 rainfall event (68 mm), the displacements increased again (Fig. 11b). The displacements recorded by the points within
301 Area 1 may ~~be~~ related to deformations affecting the deposits placed along the steep scarp connected to the main
302 crown delimiting the DSGSD (Fig. 4).

303 - Area 2 is located in the ~~d~~Detachment sector (SW side of the DSGSD). Two measuring points (Points 1 and 2) therein
304 located (Fig. 11d) recorded a peak of displacement ~~between December 2010 and March 2011~~ of about 170 mm (Point
305 1) and 130 mm (Point 2); respectively, between December 2010 and March 2011. The ground deformations recorded by
306 these points are related to slope waste deposition due to the gravity ~~affecting~~ the coarse material infilling this sector,
307 such as ancient rock avalanche deposits (Point 1) and detensioned rock mass portions (Point 2) (Fig. 4).

308 - Area 3 represents the border between ~~d~~Detachment and ~~d~~Dismantling sectors, and is located upstream of the 2010
309 event scarp (Fig. 11c). Its kinematics is represented by Point 5 behaviour, showing a trend similar to P1, which may be
310 associated with the sliding of the partly cemented and stabilized detrital cover material ~~material infilling the materials,~~
311 showing a similar trend with respect to P1 (Figs. 4-11d).

312 - Area 4 represents the lowermost portion of ~~d~~Dismantling sector. Three measuring points are therein located: Points 7,
313 8 and 9 (Figs. 11e and 11f). Points 7 and 8 display the kinematics the detrital cover surrounding the 2010 debris flow
314 triggering area. Both control points show acceleration periods alternating with ~~of~~ periods of stability. In particular the
315 trend of P8, located near the Rotolon creek ephemeral springs and channels (Frodella et al., 2014; 2015) shows a
316 correlation with cumulative precipitation above a threshold value of about 100 mm (Fig. 11f), which contribute to the
317 sub-surface water circulation within the detachment sector's loose detrital cover.

318 This suggests that the recorded displacements may be associated to the spring erosion within the detrital cover. This
 319 point records the maximum displacement of the entire area (about ICD=1236 mm) monitored by GB-InSAR system of
 320 about ICD=1236 mm. The area is apparently dominated by superficial processes, such as widespread soil erosion and
 321 slope-waste deposition due to gravity. Measuring Point 9, located nearby the dismantling sector upstream limit,
 322 records cumulative displacement of 445 mm and shows an irregular trend mainly due to its location near vegetated
 323 areas (Figs. 4-119f).
 324



325
 326 **Figure 11.** Integration between geomorphological map (modified after Frodella et al., 2014), the ICD maps
 327 displacement maps of whole monitored period, and the control points displacements time series: (a) the zoom of the
 328 Area 1 shown in Figure 7d; (b) the displacements time series of P4 and P3; (c) zoom of the Area 2 and Area 3 shown in
 329 Figure 7d; (d) the displacement time series of Points 1, 2 and 5; (e) zoom of Area 4 shown in Figure 7d; (f) the
 330 displacement time series of Points 7, 8 and 9.

331 The use of GB-InSAR ICD maps and the integration with geomorphological field surveys proved its usefulness in
 332 recognizing Area 4 (located within the DSGSD dismantling sector; Figs. 3 and 7) as the most hazardous sector within
 333 the monitored scenario, due to the widespread and intense recorded cumulated displacements (2437 mm), and its

334 geomorphological features (steep slope, loose very coarse debris and ~~acting widespread~~ surface ~~widespread~~-erosional
335 processes in act due to the presence of ephemeral springs), and frequency of reactivations (Fig. 10).

336 The main triggering factor for these shallow remobilizations ongoing in this area ~~shallow remobilizations are~~ intense
337 rainfall events, as highlighted by measuring point 8 time series (Fig. 8). Area 3 (recording 960 mm of total cumulated
338 displacements) falls as well within the Dismantling sector detrital cover, and was considered the second most hazardous
339 landslide sector within the monitored scenario.

340 Other areas characterized by relevant residual cumulated displacement were identified in Area 1 (737 mm) and Area 2
341 (751 mm), corresponding to the material infilling the Detachment sector (Fig. 2), but they were not considered
342 hazardous due to a 300 meter long and 20 meter high N-S trending trench acting as a physical barrier separating the
343 upper ~~d~~Detachment sector from the lowermost ~~d~~Dismantling sector.

344 Furthermore the comparison amongst the MCD maps (Fig. 9 and 10) highlighted widespread and frequent residual
345 displacements taking place in ~~correspondence of~~ Area 4 during the wet autumn-winter-fall months (December
346 2010=232 mm; January 2011=214 mm; March 2011=173 mm; November 2011, 2012=-174 and 106 mm respectively).
347 Nevertheless, in May 2011 Area 4 reached the highest ~~stf~~ MCD in the monitored period (244 mm), although concentrated
348 in a limited sector located near ~~by~~ the measuring Point 8 (Fig. 9d).

349 A simplified local scale early warning system (Intrieri et al., 2012) was implemented based on three different warning
350 levels: ordinary, pre-alarm and alarm levels (Figure 5). In order to ensure the safety ~~offor~~ the post-recovery
351 management personnel, hourly displacement thresholds were adopted: the level change occurred if the following
352 thresholds were surpassed (i) ordinary: <1 mm/h ~~ordinary~~; ii) pre-alarm: ~~between~~ 1.0 mm/h ~~to~~ and 5.0 mm/h ~~for the pre-~~
353 alarm; iii) alarm level: >5 mm/h ~~for the alarm level~~). Communication, which is a fundamental issue of every early
354 warning system (Intrieri et al. 2013), was operated through the dispatch of monitoring bulletins every week and
355 whenever the warning thresholds were exceeded. In this framework, based on the surface of the deformation areas and
356 the increasing trends of displacement time series, 4 monitoring alerts were obtained: i) March 19th 2011; ii) April 7th
357 2011; iii) 8-12th November 2011; iv) November 10-12th 2012 (Fig. 6). All these events were located in the area
358 monitored by measuring Point 8. Inspections carried out by the optical monitoring device and by means of field surveys
359 from safe viewing points, assessed that the detected accelerations did not generate significant slope failures, although
360 rainfall comparable to that of November 2010 had hit the area. Following the second alert, a weekly bulletin phase
361 (May 2011 - September 2012) was planned for a residual risk prevention strategy.

362

363 7. Conclusions

364 In the ~~framework context~~ of the 2010 hazardous events affecting the Rotolon creek valley, a local scale GB-InSAR
365 system was implemented for: i) mapping and monitoring slope landslide residual deformations; ~~and for ii)~~ early
366 warning purposes in case of landslide reactivations. ~~The objective, with the aim of~~ was to assuring the safety of both
367 the valley's inhabitants and the personnel involved in the post-event recovery phase. The radar system acquired GB-
368 InSAR data every 10 minutes, from which cumulated 2D displacement maps, and displacements time series of 10
369 measuring points were obtained. The analysed GB-InSAR data were uploaded both on a dedicated Web-based interface
370 and remote ftp server, allowing for: i) a daily near real time ~~data and~~ on-routine data visualization; ii) ~~and~~ on demand
371 analysis in case of critical weather events. In this ~~context framework~~, based on the surface of the deformation areas and
372 the increasing trends of displacement time series, 4 monitoring alerts were obtained and a 16 months ~~s~~ weekly monitoring
373 bulletin campaign was performed (May 2011-September 2012). All of the monitoring data were shared with the
374 technical stakeholders and decision makers involved in the emergency management. ~~The adopted monitoring system~~

375 ~~provided all of the technical personnel and the local authorities decision makers involved in the post crisis management~~
376 ~~activities with a reliable, rapid and easy communication system of the monitoring results, designed in favour of an~~
377 ~~enhanced understanding of such a critical landslide scenario and an improvement of decision making process. Based on~~
378 Given the recorded residual deformations, four critical sectors were identified in the monitored scenario, on the basis of
379 the measured cumulated displacements, frequency of activation and geomorphological features. Amongst these sectors
380 Area 3 and in particular Area 4 (recording respectively 960 mm and 2437 mm of total cumulated displacements) were
381 considered the most hazardous for potential debris flow reactivations. The latter areas are in fact located within a steep
382 landslide sector characterized by loose detrital cover, affected by soil erosion and slope-waste deposition (Dismantling
383 sector). The displacement time series of the GB-InSAR measuring points provided information on the landslide
384 kinematics: displacements range from 337 mm (Point 6) to 1476 mm (Point 8). This latter point displays the monitored
385 area's cumulated peak displacements, showing two acceleration periods (~~middle~~ March 2011 and beginning of
386 November 2011) triggered by intense precipitations, alternating with a more linear trend. The kinematics of the other
387 representative measuring points, is related either to deformations affecting the deposits placed along the steep scarp
388 connected to the main DSGSD (Points 3-4), or to slope waste deposition due to gravity affecting the coarse material
389 infilling the Detachment sector (Points 1-2-5).

390 The comparison amongst the MCD maps highlighted a first phase of widespread residual displacements (December
391 2010). In the following period, ground deformation took place in ~~correspondence of~~ limited sectors within Area 4,
392 except for a widespread reactivation recorded in November 2011. The acquired radar data suggest a complex nature of
393 the monitored landslide: its geomorphological features (e.g., rough topography, stepped profile in its upper sector,
394 showing scarps, counterscarps, ridges, trenches and ~~counterslopes~~ counter slopes, toe bulging) documents the activity of
395 deep-seated long-term ~~deep-seated~~ processes, while ~~the~~ radar data also recorded the wide spectrum of short-term
396 secondary instability phenomena, probably ~~in terms~~ related to erosional-depositional gravitational processes
397 (~~d~~Detachment sector), and soil erosion/slope-waste deposition (~~d~~Dismantling sector). Although this latter sector
398 represents the most hazardous area within the landslide phenomena, the displacements ~~therein~~ acting therein during ~~in~~ the
399 analysed time span, appear to be related to ephemeral spring erosion located within the loose detrital cover. This
400 suggests that these processes are only the surficial and secondary expression of a more complex deep-seated landslide
401 system.

402 The monitoring system adopted provided all of the technical personnel and decision-making local authorities involved
403 in the post-crisis management activities with a reliable, rapid and easy communication system of the results of the
404 monitoring campaign. This favoured an enhanced understanding of such a critical landslide scenario (a populated
405 mountainous area particularly devoted to touristic activities), during the post-emergency management activities. The
406 here presented methodology could represent a useful contribution for a better understanding of landslide phenomena
407 and decision making process during the post-emergency management activities in a critical landslide scenario (a
408 populated mountainous area particularly devoted to touristic activities). Furthermore, the methodology could be
409 profitably adapted, modified, and updated in other geological contexts.

410

411 **Acknowledgements**

412 The GB-InSAR apparatus used in this application was designed and produced by Ellegi s.r.l., and based on the
413 proprietary LiSALAB GB-InSAR technology, derived from the evolution and improvement of LiSA technology

414 | [\(licensed by the Ispra Joint Research Centre of the European Commission\)](#). We also would like to thank the Veneto Soil
415 | Defence Regional Direction for providing Lidar and aerial photo data.

416 | **References**

- 417 | Abellán, A., Vilaplana, J.M. and Martínez, J.: Application of a long-range terrestrial laser scanner to a detailed rockfall
418 | study at Vall de Núria (Eastern pyrenees, Spain), *Eng. Geol.*, 88, 136–148, 2006.
- 419 | Agliardi, F., Crosta, G. and Zanchi A.: Structural constraints on deep-seated slope deformation kinematics. *Eng. Geol.*,
420 | 59, 1-2, 83-102, 2001.
- 421 | Antonello, G., Casagli, N., Farina, P., Leva, D., Nico, G., Sieber, A.J. and Tarchi D.: Ground-based SAR interferometry
422 | for monitoring mass movements, *Landslides*, 1, 21–28, 2004.
- 423 | Bamler, R. and Hartl, P.: Synthetic aperture radar interferometry, *Inverse Probl.*, 14, 1–54, 1998.
- 424 | Bardi, F., Frodella, W., Ciampalini, A., Bianchini, S., Del Ventisette, C., Gigli, G., Fanti, R., Moretti, S., Basile, G. and
425 | Casagli, N.: Integration between ground based and satellite SAR data in landslide mapping: the San Fratello case study,
426 | *Geomorphology*, 223, 45-60, 2014.
- 427 | Bardi, F., Raspini, F., Frodella, W., Lombardi, L., Nocentini, M., Gigli, G., Morelli, S., Corsini, A. and Casagli, N.:
428 | Monitoring the Rapid-Moving Reactivation of Earth Flows by Means of GB-InSAR: The April 2013 Capriglio
429 | Landslide (Northern Appennines, Italy), *Remote Sensing*, 9(2), 165, 2017a.
- 430 | Bardi, F., Raspini, F., Frodella, W., Lombardi, L., Nocentini, M., Gigli, G., Morelli, S., Corsini, A. and Casagli, N.:
431 | Remote sensing mapping and monitoring of the Capriglio landslide (Parma Province, northern Italy). In Mikos, M.,
432 | Arbanas, Ž., Yin, Y., Sassa, K. (Eds) *Advancing culture of living with landslides, Vol 3 - Advances in Landslide*
433 | *Technology*, Springer International Publishing, Switzerland, pp 231-238. Doi: 10.1007/978-3-319-53487-9_26, 2017b.
- 434 | Bertolaso, G., De Bernardinis, B., Bosi, V., Cardaci, C., Ciolli, S., Colozza, R., Cristiani, C., Mangione, D., Ricciardi,
435 | A., Rosi, M., Scalzo, A. and Soddu P.: Civil protection preparedness and response to the 2007 eruptive crisis of
436 | Stromboli volcano, Italy, *Journal of Volcanology and Geothermal Research*, 182, 269–277, 2009.
- 437 | [Bossi, G., Crema, S., Frigerio, S., Mantovani, M., Marcato, G., Pasuto A., Schenato L., Marco Cavalli M.: The Rotolon](#)
438 | [catchment early-warning system. In: Lollino G et al. \(eds.\), *Engineering Geology for Society and Territory*. Springer](#)
439 | [International Publishing 3: 91-95, 2015. DOI: 10.1007/978-3-319- 09054-2 18.](#)
- 440 | Broussolle, J., Kyovtorov, V., Basso, M., Ferraro Di Silvi, E., Castiglione, G., Figueiredo Morgado, J., Giuliani, R.,
441 | Oliveri, F., Sammartino, P.F. and Tarchi, D.: MELISSA, a new class of ground based InSAR system. An example of
442 | application in support to the Costa Concordia, *ISPRS J. Photogramm. Remote Sens*, 91, 50–58, 2014.
- 443 | Carlà, T., Intrieri, E., Di Traglia, F. and Casagli, N.: A statistical-based approach for determining the intensity of unrest
444 | phases at Stromboli volcano (Southern Italy) using one-step-ahead forecasts of displacement time series, *Natural*
445 | *Hazards*, 84(1), 669-683, 2016.
- 446 | Carlà, T., Intrieri, E., Di Traglia, F., Nolesini, T., Gigli, G. and Casagli, N.: Guidelines on the use of inverse velocity
447 | method as a tool for setting alarm thresholds and forecasting landslides and structure collapses, *Landslides*, 14, (2),
448 | 517–534, 2017.
- 449 | Casagli N, Catani F, Del Ventisette C and Luzi G (2010) Monitoring, prediction, and early warning using ground-based
450 | radar interferometry. *Landslides* 7(3):291-301.
- 451 | Casagli, N., Frodella, W., Morelli, S., Tofani, V., Ciampalini, A., Intrieri, E., Raspini, F., Rossi, G., Tanteri, L. and Lu,
452 | P.: Spaceborne, UAV and ground-based remote sensing techniques for landslide mapping, monitoring and early
453 | warning. *Geoenvironmental Disasters* 4(9) DOI 10.1186/s40677-017-0073-1, 2017a.

454 Casagli, N., Tofani, V., Morelli, S., Frodella, W., Ciampalini, A., Raspini, F., and Intrieri, E.: Remote Sensing
455 Techniques in Landslide Mapping and Monitoring, Keynote Lecture. In Mikos, M., Arbanas, Ž., Yin, Y., Sassa, K.
456 (Eds) Advancing culture of living with landslides, Vol 3 – Advances in Landslide Technology, Springer International
457 Publishing, Switzerland, pp 1-19. doi: 10.1007/978-3-319-53487-9_1, 2017b.

458 [Casu, F., Manzo, M., Lanari, R. \(2006\). A quantitative assessment of the SBAS algorithm performance for surface
459 deformation retrieval from DInSAR data. Remote Sensing of Environment., 102 \(3-4\), 195-210.](#)

460 Chandler, J.: Effective application of automated digital photogrammetry for geomorphological research, Earth Surface
461 Processes and Landforms, 24, 51–63, 1999.

462 Ciampalini, A., Raspini, F., Bianchini, S., Frodella, W., Bardi, F., Lagomarsino, D., Di Traglia, F., Moretti, S., Proietti,
463 C., Pagliara, P., Onori, R., Corazza, A., Duro, A., Basile, G. and Casagli, N.: Remote sensing as tool for development of
464 landslide databases: The case of the Messina Province (Italy) geodatabase, Geomorphology, 249, 103-118, 2015.

465 Ciampalini A, Raspini F, Frodella W, Bardi F, Bianchini S, Moretti S. (2016) The effectiveness of high-resolution
466 LiDAR data combined with PSInSAR data. Landslides, 13 (2), 399-410.

467 Confuorto, P., Di Martire, D., Centolanza, G., Iglesias, R., Mallorqui, J.J., Novellino, A., Plank, S, Ramondini, M.,
468 Thuro, K. and Calcaterra, D.: Post-failure evolution analysis of a rainfall-triggered landslide by multi-temporal
469 interferometry SAR approaches integrated with geotechnical analysis. Remote Sensing of Environment, 188, 51-72,
470 2017.

471 Crosta G.B. (1996) - Landslide, spreading, deep seated gravitational deformation: Analysis, examples, problems and
472 proposals. Geografia Fisica e Dinamica Quaternaria, 19: 297–313.

473 Crosta, G.B. and Agliardi, F.: Failure forecast for large rock slides by surface displacement measurements. Canadian
474 Geotechnical Journal, 40(1), 176–191, 2003.

475 Cruden, D.M., and Varnes, D.J.: Landslides Types and Processes. In: Turner AK, Schuster RL (eds.), Landslides:
476 Investigation and Mitigation. Transportation Research Board Special Report 247, National Academy Press, WA, 36–75,
477 1996.

478 Del Soldato, M., Segoni, S., De Vita, P., Pazzi, V., Tofani, V., Moretti, S.: Thickness model of pyroclastic soils along
479 mountain slopes of Campania (southern Italy). In: Aversa et al. (Eds.). Landslides and Engineered Slopes. Experience,
480 Theory and Practice. Associazione Geotecnica Italiana, Rome, Italy. ISBN:978-1-138-02988-0, 2016

481 Del Ventisette, C., Intrieri, E., Luzi, G., Casagli, N., Fanti, R. and Leva, D.: Using ground based radar interferometry
482 during emergency: The case of the A3 motorway (Calabria Region, Italy) threatened by a landslide, Natural Hazards
483 and Earth System Science, 11(9), 2483-2495, 2011.

484 De Zanche V., Mietto P. (1981). Review of the Triassic sequence of Recoaro (Italy) and related problems. Rend. Soc.
485 Geol. It., Padova. 25-28.

486 Di Traglia, F., Intrieri, E., Nolesini, T., Bardi, F., Del Ventisette, C., Ferrigno, F., Frangioni, S., Frodella, W., Gigli, G.,
487 Lotti, A., Tacconi Stefanelli, C., Tanteri, L., Leva, D. and Casagli N.: The ground-based InSAR monitoring system at
488 Stromboli volcano: Linking changes in displacement rate and intensity of persistent volcanic activity, Bulletin of
489 volcanology, 76(2), 786, 2014a.

490 Di Traglia F., Nolesini, T., Intrieri, E., Mugnai, F., Leva, D., Rosi, M. and Casagli N.: Review of ten years of volcano
491 deformations recorded by the ground-based InSAR monitoring system at Stromboli volcano: a tool to mitigate volcano
492 flank dynamics and intense volcanic activity, Earth-Sci. Rev., 139, 317–335, 2014b.

493 Di Traglia, F., Battaglia, M., Nolesini, T., Lagomarsino, D. and Casagli N.: Shifts in the eruptive styles at Stromboli in
494 2010–2014 revealed by ground-based InSAR data, Scientific Reports, 5, 13569, 2015.

495 Fidolini, F., Pazzi, V., Frodella, W., Morelli, S. and Fanti, R.: Geomorphological characterization, monitoring and
496 modeling of the Monte Rotolon complex landslide (Recoaro terme, Italy), *Engineering Geology for Society and*
497 *Territory*, 2, 1311-1315. Springer International Publishing, 2015.

498 [Frigerio, S., Schenato, L., Bossi, G., Cavalli, M., Mantovani, M., Marcato, G., Pasuto, A.: A web-based platform for](#)
499 [automatic and continuous landslide monitoring: The Rotolon \(Eastern Italian Alps\) case study. *Computers &*](#)
500 [Geosciences 63: 96-105, 2014. DOI: 10.1016/j.cageo.2013.10.015.](#)

501 Frodella, W., Morelli, S., Fidolini, F., Pazzi, V. and Fanti R.: Geomorphology of the Rotolon landslide (Veneto region,
502 Italy), *Journal of Maps*, 10(3), 394-401, 2014.

503 Frodella, W., Fidolini, F., Morelli, S. and Pazzi, F.: Application of Infrared Thermography for landslide mapping: the
504 Rotolon DSGDS case study, *Rend. Online Soc. Geol. It.*, 35, 144-147, 2015.

505 Frodella, W., Ciampalini, A., Gigli, G., Lombardi, L., Raspini, F., Nocentini, M., Scardigli, C. and Casagli, N.:
506 Synergic use of satellite and ground based remote sensing methods for monitoring the San Leo rock cliff (Northern
507 Italy), *Geomorphology* 264:80-94, 2016.

508 Frodella, W., Morelli, S. and Pazzi, V.: Infrared Thermographic surveys for landslide mapping and characterization: the
509 Rotolon DSGSD (Northern Italy) case study, *Italian Journal of Engineering Geology and Environment*. Accepted in
510 press. DOI: 10.4408/IJEGE.2017-01.S-07, 2017.

511 Gigli, G., Frodella, W., Mugnai, F., Tapete, D., Cigna, F., Fanti, R., Intrieri, E. and Lombardi L.: Instability
512 mechanisms affecting cultural heritage sites in the Maltese Archipelago, *Nat. Hazards Earth Syst. Sci.* 12:1-2, 2012.

513 Gigli, G., Intrieri, E., Lombardi, L., Nocentini, M., Frodella, W., Balducci, M., Venanti, L.D. and Casagli, N.: Event
514 scenario analysis for the design of rockslide countermeasures, *J. Mt. Sci.*, 11(6), 1521–1530, 2014a.

515 Gigli, G., Frodella, W., Garfagnoli, F., Mugnai, F., Morelli, S., Menna, F. and Casagli, N.: 3-D geomechanical rock
516 mass characterization for the evaluation of rockslide susceptibility scenarios, *Landslides*, 11(1), 131-140, 2014b.

517 Gigli, G., Morelli, S., Fornera, S., and Casagli, N.: Terrestrial laser scanner and geomechanical surveys for the rapid
518 evaluation of rock fall susceptibility scenarios. *Landslides*, 11(1), 1-14, 2014c.

519 [Gullà, G., Peduto, D., Borrelli, L., Antronico, L., Fornaro, G.-\(2017\). Geometric and kinematic characterization of](#)
520 [landslides affecting urban areas: the Lungro case study \(Calabria, Southern Italy\). *Landslides* 14:171–188, 2017.](#)
521 [doi:10.1007/s10346-015-0676-0.](#)

522 Guzzetti, F., Mondini, A.C., Cardinali, M., Fiorucci, M., Santangelo, M. and Chang, K.T.: Landslide inventory maps:
523 new tools for an old problem, *Earth Science Reviews*, 112, 1–25, 2012.

524 Intrieri, E., Gigli, G., Mugnai, F., Fanti, R. and Casagli, N.: Design and implementation of a landslide early warning
525 system, *Engineering Geology*, 147, 124-136, 2012.

526 Intrieri, E., Gigli, G., Casagli, N. And Nadim, F.: Brief communication" Landslide Early Warning System: toolbox and
527 general concepts", *Natural hazards and earth system sciences*, 13(1), 85-90, 2013.

528 Jaboyedoff, M., Oppikofer, T., Abellán, A., Derron, M.H., Loya, A., Metzger, R. and Pedrazzini, A.: Use of LIDAR in
529 landslide investigations: a review, *Natural hazards*, 61(1), 5-28, 2012.

530 Lombardi, L., Nocentini, M., Frodella, W., Nolesini, T., Bardi, F., Intrieri, E., Carlà, T., Solari, L., Dotta, G., Ferrigno,
531 F. and Casagli, N.: The Calatabiano landslide (southern Italy): preliminary GB-InSAR monitoring data and remote 3D
532 mapping, *Landslides*:1-12, 2017.

533 Lotti, A., Saccorotti, G., Fiaschi, A., Matassoni, L., Gigli, G., Pazzi, V. and Casagli, N.: Seismic monitoring of
534 rockslide: the Torgiovanetto quarry (Central Apennines, Italy), in: G. Lollino et al. (eds), *Engineering Geology for*

535 Society and Territory – Vol.2, Springer International Publishing, Switzerland, 1537-1540, doi: 10.1007/978-3-319-
536 09057-3_272, 2015.

537 Luzi, G., Pieraccini, M., Mecatti, D., Noferini, L., Guidi, G., Moia, F. and Atzeni, C.: Ground-based radar
538 interferometry for landslides monitoring: atmospheric and instrumental decorrelation sources on experimental data,
539 IEEE Trans. Geosci. Remote Sens, 42(11), 2454–2466, 2004.

540 Luzi, G.: Ground Based SAR Interferometry: a novel tool for geosciences, P. Imperatore, D. Riccio (Eds.), Geoscience
541 and Remote Sensing. New Achievements, InTech, 1-26, 2010.

542 Monserrat, O., Crosetto, M. and Luzi, G.: A review of ground-based SAR interferometry for deformation
543 measurement, ISPRS Journal of Photogrammetry and Remote Sensing 93, 40-48, 2014.

544 Morelli, S., Pazzi, V., Monroy, V. H. G., and Casagli, N.: Residual Slope Stability in Low Order Streams of Anganguero
545 Mining Area (Michoacán, Mexico) After the 2010 Debris Flows. In Mikos, M., Casagli, N., Yin, Y., Sassa, K. (Eds)
546 Advancing culture of living with landslides, Vol 4 – Diversity of landslide forms, Springer International Publishing,
547 Switzerland, pp 651-660. doi: 10.1007/978-3-319-53485-5_75, 2017.

548 [Nicodemo G, Peduto D, Ferlisi S, Maccabiani J.-\(2016\). Investigating building settlements via very high resolution](#)
549 [SAR sensors. In: Bakker J, Frangopol D.M., van Breugel K \(eds\) © 2017Life-cycle of engineering systems: emphasis](#)
550 [on sustainable Civil Infrastructure. Taylor & Francis Group, London, pp 2256–2263, 2016.](#)

551 Nolesini, T., Di Traglia, F., Del Ventisette, C., Moretti, S. and Casagli, N.: Deformations and slope instability on
552 Stromboli volcano: Integration of GBInSAR data and analog modeling, Geomorphology 180, 242-254, 2013.

553 Nolesini T, Frodella W, Bianchini S and Casagli, N.: Detecting Slope and Urban Potential Unstable Areas by Means of
554 Multi-Platform Remote Sensing Techniques: The Volterra (Italy) Case Study, Remote Sensing, 8(9), 746, 2016.

555 Pagliara, P., Basile, G., Cara, P., Corazza, A., Duro, A., Manfrè, B., Onori, R., Proietti, C. and Sansone, V.: Integration
556 of earth observation and ground-based HR data in the civil protection emergency cycle: the case of the DORIS project,
557 in: Pardo-Igúzquiza E, Guardiola-Albert C, Heredia J, Moreno-Merino L, Durán JJ, Vargas-Guzmán JA (Eds.)
558 Mathematics of Planet Earth, Lecture Notes in Earth System Sciences. Springer, Berlin Heidelberg 263–266, 2014.

559 Pazzi, V., Tanteri, L., Bicocchi, G., Caselli, A., D'Ambrosio, M., Fanti, R.: H/V technique for the rapid detection of
560 landslide slip surface(s): assessment of the optimized measurements spatial distribution. In Mikos, M., Tiwari, B., Yin,
561 Y., Sassa, K. (Eds) Advancing culture of living with landslides, Vol 2 – Advances in landslide science, Springer
562 International Publishing, Switzerland, pp 335-343. doi: 10.1007/978-3-319-53498-5_38. 2017a

563 Pazzi, V., Tanteri, L., Bicocchi, G., D'Ambrosio, M., Caselli, A., and Fanti, R.: H/V measurements as an effective tool
564 for the reliable detection of landslide slip surfaces: Case studies of Castagnola (La Spezia, Italy) and Roccalbegna
565 (Grosseto, Italy), Physics and Chemistry of the Earth, 98, 136-153, doi: <http://dx.doi.org/10.1016/j.pce.2016.10.014>,
566 2017b.

567 [Peduto D., Ferlisi S., Nicodemo G., Reale D., Pisciotta G., Gullà G.-\(2017a\). Empirical fragility and vulnerability](#)
568 [curves for buildings exposed to slow-moving landslides at medium and large scales, Landslides, in press, 2017a. DOI :](#)
569 [10.1007/s10346-017-0826-7.](#)

570 [Peduto, D, Nicodemo, G, Maccabiani, J, Ferlisi, S.-\(2017b\). Multi-scale analysis of settlement induced building damage](#)
571 [using damage surveys and DInSAR data: a case study in The Netherlands. Engineering Geology, 218:117–133, 2017b.](#)
572 [doi:10.1016/j.enggeo.2016.12.018.](#)

573 Pieraccini, M., Tarchi, D., Rudolf, H., Leva, D., Luzi, G., Bartoli, G. and Atzeni, C.: Structural static testing by
574 interferometric synthetic radar, NDT and E Intl., 33(8), 565–570, 2000.

575 Pieraccini, M., Casagli, N., Luzi, G., Tarchi, D., Mecatti, D., Noferini, L. and Atzeni, C.: Landslide monitoring by
576 ground-based radar interferometry: a field test in Valdarno (Italy), *Int J Remote Sens* 24:1385–1391, 2002.

577 Salvatici, T., Morelli, S., Pazzi, V., Frodella, W. and Fanti, R.: Debris flow hazard assessment by means of numerical
578 simulations: implications for the Rotolon Creek Valley (Northern Italy), *Journal of Mountain Science*, 14 (4), 636-648,
579 DOI:10.1007/s11629-016-4197-7, 2017.

580 Tarchi, D., Ohlmer, E. and Sieber, A.J.: Monitoring of structural changes by radar interferometry, *Res. Nondestruct.*
581 *Eval.* 9, 213–225, 1997.

582 Tarchi, D., Casagli, N., Fanti, R., Leva, D., Luzi, G., Pasuto, A., Pieraccini, M. and Silvano, S.: Landslide monitoring
583 by using ground-based SAR interferometry: an example of application to the Tessina landslide in Italy, *Engineering*
584 *Geology*, 68, 15-30, 2003.

585 Tapete, D., Gigli, G., Mugnai, F., Vannocci, P., Pecchioni, E., Morelli, S., Fanti R., and Casagli, N.: Correlation
586 between erosion patterns and rockfall hazard susceptibility in hilltop fortifications by terrestrial laser scanning and
587 diagnostic investigations. In: *IEEE International Geoscience and Remote Sensing Symposium. Remote Sensing for a*
588 *Dynamic Earth*. Munich, Germany, 22-27 July 2012, pp. 4809-4812. ISBN 978-1-4673-1159-5, 2012.

589 [Tofani, V., Raspini, F., Catani, F., Casagli, N., Persistent scatterer interferometry \(PSI\) technique for landslide](#)
590 [characterization and monitoring. In: Sassa, K., Canuti, P., Yueping, Y. \(Eds.\), *Landslide Science for a Safer*](#)
591 [Geoenvironment Methods of Landslide Studies 2. Springer International Publishing, pp. 351–357 \(ISBN:](#)
592 [9783319050492\).](#) 2014.

593 Zischinsky, U.: Uber sackungen, *Rock Mech.*, 1(1), 30–52, 1969.

594 Zhang, Z., Zheng, S. and Zhan, Z.: Digital terrestrial photogrammetry with photo total station, *International Archives of*
595 *Photogrammetry and Remote Sensing*, Istanbul, Turkey, 232-236, 2004.